

## Pion and $\rho$ -meson form factors using four-point functions in $N_F=2$ QCD

---

**Constantia Alexandrou**

*University of Cyprus, Department of Physics, P.O.Box 20537, 1678 Nicosia, Cyprus*

*E-mail: alexand@ucy.ac.cy*

**Giannis Koutsou\***

*University of Cyprus, Department of Physics, P.O.Box 20537, 1678 Nicosia, Cyprus*

*E-mail: koutsou@ucy.ac.cy*

Hadron wave functions and form factors can be extracted using four-point correlators. Stochastic techniques are used to estimate the all to all propagators, which are required for the exact calculation of four-point functions. We apply the so called one-end trick to evaluate meson four-point functions. We demonstrate the effectiveness of the technique in the case of the pion and the  $\rho$ -meson where we extract their charge distribution, as well as the form factors.

*The XXV International Symposium on Lattice Field Theory*

*July 30-4 August 2007*

*Regensburg, Germany*

---

\*Speaker.

## 1. Introduction

The standard approach used in the evaluation of form factors in lattice QCD is to compute a three-point function. More detailed information on hadron structure can be extracted from four-point correlators. The quark distribution inside the hadron and hadron deformation are just two such important aspects that can be studied using these correlators. The equal time density-density correlator provides a gauge invariant definition of the hadron "wave function" but originally could only be evaluated approximately [1]. This is because four-point functions are harder to compute than two- and three-point functions, requiring the all to all propagator. The usual way to estimate the all to all propagator is by employing stochastic techniques [2]. In Ref [3, 4] we used  $Z(2)$  noise combined with dilution to compute the all to all propagators and obtained results both for mesons and baryons [3, 4]. In this work we generalize the so called one-end trick [5], originally devised as a method to calculate two-point functions, to evaluate four-point functions. We demonstrate that this approach yields more accurate results by evaluating the density-density correlator for the pion and  $\rho$ -meson and comparing the results to those obtained using standard stochastic techniques [3, 4]. Furthermore, we extract the pion form factor obtaining results that have comparable errors as those obtained when one uses the one-end trick to compute the pion form factor using the three-point function [6]. An advantage of using four-point functions is that we only need one set of stochastic propagators to extract the form factor for *any* momentum transfer unlike using three-point functions where a new set is needed for every momentum. We also show how to generalize our method to other mesons and give preliminary results on  $G_1$ , one of the three form factors of the  $\rho$ -meson.

## 2. Four-point functions

Hadron four-point functions are given by

$$G_h^{j_\sigma}(\vec{x}_2, t_1, t_2) = \int d^3x_1 d^3x \langle h(\vec{x}, t) | j_\sigma^{q_f}(\vec{x}_2 + \vec{x}_1, t_2) j_\sigma^{q_{f'}}(\vec{x}_1, t_1) | h(\vec{x}_0, t_0) \rangle \quad (2.1)$$

where  $j_\sigma^{q_f}$  is the normal ordered electromagnetic operator :  $\bar{q}_f \gamma_\sigma q_f$  : with  $f$  being a flavor index, while  $|h\rangle$  denotes any hadronic state. The two integrations ensure zero momentum of the hadronic state; integrating over  $\vec{x}_1$  sets the momentum of the source equal to that of the sink and integrating over  $\vec{x}$  sets both to zero. Thus to compute the four-point function on the lattice, the all to all propagator from all sites  $\vec{x}_1$  to  $\vec{x}$  is needed.

It is well known that an estimate for the all to all propagator can be obtained using stochastic techniques [2]. In brief, one inverts for a set of  $N_r$  noise vectors obeying  $\langle \xi_\mu^a(x) \xi_\nu^{b\dagger}(y) \rangle_r = \delta(x - y) \delta_{a,b} \delta_{\mu,\nu}$  and  $\langle \xi_\mu^a(x) \rangle_r = 0$  and estimates the all to all propagator by averaging the product of the solution vectors with the noise vectors over the stochastic ensemble. Namely the quark propagator  $G_{v,\mu}^{b,a}(x, y) \rightarrow \langle \phi_v^b(x) \xi_\mu^{a\dagger}(y) \rangle_r$ , where  $\xi$  is a noise vector and  $\phi$  the solution vector. One, therefore, replaces every occurrence of  $G$  with the product between  $\xi$  and  $\phi$  thereby obtaining the stochastic estimate for the four-point function. More details and results for hadron wave functions and the pion form factor obtained using this method can be found in Refs. [3, 4], where it is shown that with sufficient number of noise vectors and dilution one can obtain a reasonable signal [7]. We shall refer to this approach as Method I. Here we show how one can reduce stochastic noise by implementing the one-end trick [5] for the computation of meson four-point functions. We shall refer to this new approach as Method II.

### 3. Description of Method II

The one-end trick was originally devised for the precise calculation of pion two-point functions. In its original form, one combines appropriately solution vectors so that an automatic summation over the source coordinate arises. Thus the number of stochastic inversions needed is reduced to a few inversions, thereby suppressing stochastic noise. More explicitly, expanding the dot product between two solution vectors yields the pion two-point correlator summed over the source coordinate:

$$\sum_{\vec{x}} \langle \phi_{\mu}^{\dagger a}(\vec{x}, t) \phi_{\mu}^a(\vec{x}, t) \rangle_r = \sum_{\vec{x}, \vec{y}_0, \vec{x}_0} \left\langle \left[ G_{\mu\nu}^{ab}(\vec{x}, t; \vec{x}_0, t_0) \xi_{\nu}^b(\vec{x}_0, t_0) \right]^{\dagger} G_{\mu\nu'}^{ab'}(\vec{x}, t; \vec{x}_0, t_0) \xi_{\nu'}^{b'}(\vec{y}_0, t_0) \right\rangle_r, \quad (3.1)$$

where we assume that the noise vectors are localized on a certain time slice  $t_0$ . Taking the average of the noise vectors over the stochastic ensemble yields  $\delta$ -functions by definition. Thus we obtain

$$\sum_{\vec{x}, \vec{y}_0, \vec{x}_0} \left[ G_{\mu\nu}^{ab}(\vec{x}, t; \vec{x}_0, t_0) \right]^{\dagger} G_{\mu\nu'}^{ab'}(\vec{x}, t; \vec{y}_0, t_0) \delta_{aa'} \delta_{\nu\nu'} \delta(\vec{x}_0 - \vec{y}_0) = \sum_{\vec{x}, \vec{x}_0} Tr \left[ |G(\vec{x}, t; \vec{x}_0, t_0)|^2 \right]. \quad (3.2)$$

In the case of the pion Eq. (3.2) arises automatically since one combines the backward going propagator with the  $\gamma_5$  pairs that appear in the pion interpolating operator. For a general interpolating field, say  $\bar{q}_i \Gamma q_j$ , where  $\Gamma$  is any product of  $\gamma$ -matrices, the noise vectors must be diluted in spin i.e.  $\xi_{\mu}^a(\vec{x}_0, t_0)_r = \xi^a(\vec{x}_0, t_0) \delta_{r\mu}$ ,  $r = 1, \dots, 4$ . This imposes that the number of noise vectors is in multiplets of four. In this case the solution vectors give  $\phi_{\mu}^a(\vec{x}, t; t_0)_r = \sum_{\vec{x}_0} G_{\mu r}^{ab}(\vec{x}, t; \vec{x}_0, t_0) \xi^b(\vec{x}_0, t_0)$ , where the  $t_0$  argument appearing in  $\phi$  is to remind us that the noise vector is localized on the time slice  $t_0$ . The combination given by

$$\sum_{r, \vec{x}} \phi_{\mu}^a(\vec{x}, t; t_0)_r (\Gamma \gamma_5)_{\nu r} \phi_{\kappa}^{*a}(\vec{x}, t; t_0)_r (\gamma_5 \bar{\Gamma})_{\kappa \mu}, \quad (3.3)$$

yields the two-point function of the meson summed over both sink and source coordinates. The downside of this method is that, due to the automatic summation over both the source and sink spatial coordinates, one cannot compute two-point functions for arbitrary momenta using a given set of noise vectors. To utilize the one-end trick and extract the two-point correlator at finite momentum one must multiply the noise vectors with an appropriate phase prior to the inversion. Thus one needs  $N_r$  inversions for every momentum vector.

The application of this method to four-point functions is appealing since by definition (see Eq. (2.1)) one is interested in the case where the initial and final states are at rest. We show here how the one-end trick can be implemented for the case of mesons. The four-point function that we consider is shown schematically in Fig. 1. At the propagator level we have

$$G_{\Gamma}^{j\sigma}(\vec{x}_2; t_0, t_1, t_2, t) = \sum_{\vec{x}_1, \vec{x}, \vec{x}_0} \langle \chi_{\Gamma}(\vec{x}, t) | j^{\sigma}(\vec{x}_2 + \vec{x}_1, t_2) j^{\sigma}(\vec{x}_1, t_1) | \chi_{\Gamma}(\vec{x}_0, t_0) \rangle \quad (3.4)$$

$$= \sum_{\vec{x}_1, \vec{x}, \vec{x}_0} Tr \left[ \gamma_5 \gamma_{\sigma} G(\vec{x}_1, t_1; \vec{x}_0, t_0) \bar{\Gamma} \gamma_5 G^{\dagger}(\vec{x}_2 + \vec{x}_1, t_2; \vec{x}_0, t_0) \gamma_5 \gamma_{\sigma} G(\vec{x}_2 + \vec{x}_1, t_2; \vec{x}, t) \Gamma \gamma_5 G^{\dagger}(\vec{x}_1, t_1; \vec{x}, t) \right]$$

where  $\bar{\Gamma} = \gamma_0 \Gamma^{\dagger} \gamma_0$  and  $\chi_{\Gamma}(x)$  is the interpolating field of the meson that takes the general form  $\bar{q}_i(x) \Gamma q_j(x)$  for  $i \neq j$ . Here we explicitly add a sum over the source coordinate  $\vec{x}_0$  and we fix the

$\beta = 5.6, a^{-1} = 2.56(10) \text{ GeV}$			
# Confs.	$\kappa$	$am_\pi$	$m_\pi/m_\rho$
$24^3 \times 40$ [8]			
185	0.1575	0.270(3)	0.69
150	0.1580	0.199(3)	0.56
$24^3 \times 32$ [9]			
200	0.15825	0.150(3)	0.45

**Table 1:** The simulation parameters used in our computations.

time slice of the source,  $t_0$ , and the sink,  $t$ . The time slices,  $t_1$  and  $t_2$ , where the currents are inserted, on the other hand, are free to take any value between  $t_0$  and  $t$ . Thus one needs two sets of stochastic inversions, one set with the noise vectors localized on the time slice,  $t_0$  and one on the time slice,  $t$ . One then finds an appropriate combination of solution vectors such that the summation over source and sink coordinates is carried out automatically. The combination:

$$\sum_{\vec{x}_1} \text{Tr} [\gamma_5 \gamma_\sigma S(\bar{\Gamma}; \vec{x}_1, t_1; \vec{x}_2 + \vec{x}_1, t_2; t_0) \gamma_5 \gamma_\sigma S(\Gamma; \vec{x}_2 + \vec{x}_1, t_2; \vec{x}_1, t_1; t)] \quad (3.5)$$

where  $S_{\mu\nu}^{ab}(\Gamma; \vec{x}_2 + \vec{x}_1, t_2; \vec{x}_1, t_1; t) = \sum_r \phi_\mu^a(\vec{x}_2 + \vec{x}_1, t_2; t)_r (\Gamma \gamma_5)_{r\kappa} \phi_\nu^{*b}(\vec{x}_1, t_1; t)_\kappa$  achieves this.

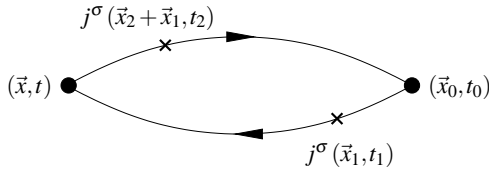


**Figure 1:** The four-point function for mesons.

Throughout this work we use two degenerate flavors of dynamical Wilson quarks [8, 9]. In all computations we employ Gaussian smearing combined with hypercubic (HYP) smearing of the gauge links that enter the Gaussian smearing function. The parameters of the Gaussian smearing are adjusted to ensure minimal time evolution for filtering the meson ground state. The parameters of our calculation are summarized in Table 1.

#### 4. Meson wave functions

The  $\rho$ -meson charge distribution is obtained using the equal time density-density correlator given by

$$G_\rho^{j_0}(\vec{x}_1, t_1) = \int d^3x_2 d^3x \langle \rho(\vec{x}, t) | j_0^{j_0}(\vec{x}_2 + \vec{x}_1, t_1) j_0^d(\vec{x}_2, t_1) | \rho(\vec{x}_0, t_0) \rangle. \quad (4.1)$$

We test the new technique by comparing results for  $G_\rho^{j_0}(\vec{x}_1, t_1)$  using Methods I and II. In the large  $t_1$  and  $t - t_1$  limit when the  $\rho$  state dominates,  $G_\rho^{j_0}(\vec{x}_1, t_1)$ , normalized over the spatial volume, becomes time independent and it is denoted by  $C_\rho(\vec{x}_1)$ . In the non-relativistic limit, this four-point function reduces to the wave function squared. The ingredients needed in Method I are the point to all propagator from the source and two all to all propagators at time slices  $t_1$  and  $t$ , both of which are kept fixed. For this computation we use six sets of noise vectors diluted for each spin, color and even-odd sites i.e. we need  $24 \times 6 = 144$  inversions to obtain each stochastic propagator. This means a total of  $144 \times 2 + 12 = 300$  inversions are required for each gauge configuration [4]. For Method II, on the other hand, we used eight sets of spin diluted noise vectors at the source and sink thus a total of 64 inversions for each configuration. In Fig. 2 we show a comparison between the results obtained using Method I and II. What is plotted is the projection of the density-density correlator,  $C_\rho(\vec{x}_1)$ , along the spin axis taken to be the z-axis and perpendicular to it. The interpolating field used for the  $\rho$ -meson is  $\bar{u}\gamma_3 d$ . As can be seen the statistical errors obtained when

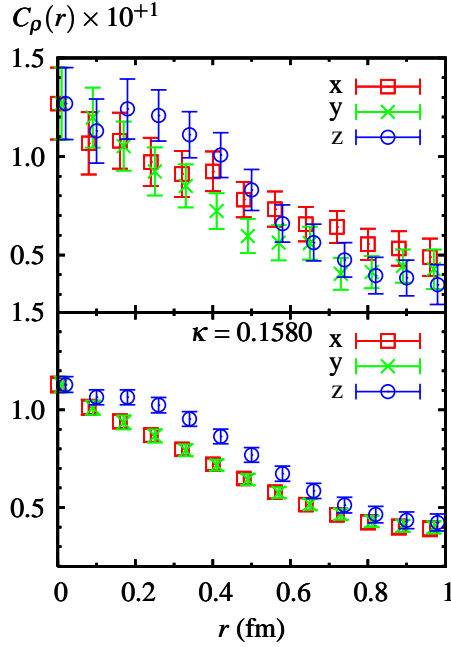


**Figure 2:** Projections of the  $\rho$ -meson density-density correlator along the spin axis and perpendicular to it. Upper for Method I and lower for Method II at  $\kappa = 0.1580$ .

using Method II are almost four times smaller despite the fact that we use  $144/32 = 4.5$  less number of noise vectors to estimate the all to all propagator. Therefore the improvement gained using the one-end trick is really significant, reducing computational time by two orders of magnitude. The results obtained in Method II clearly reveal an asymmetry in the charge distribution of the  $\rho$ -meson, which in Method I was hard to see.

Having demonstrated the effectiveness of Method II we use it, in what follows, to study deformation in the  $\rho$ -meson as a function of the quark mass and to extract the pion and  $\rho$ -meson form factors. In Fig. 3 we show contour plots of the density-density correlator of the  $\rho$ -meson,  $C_\rho(\mathbf{r})$ , projected onto the  $y$ - $z$  plane. As can be seen, for all three pion masses, we obtain an ellipse that is elongated along the spin axis, showing a clear deformation from spherical symmetry. The corresponding contour plots for the pion show no deviation from the circle as expected.

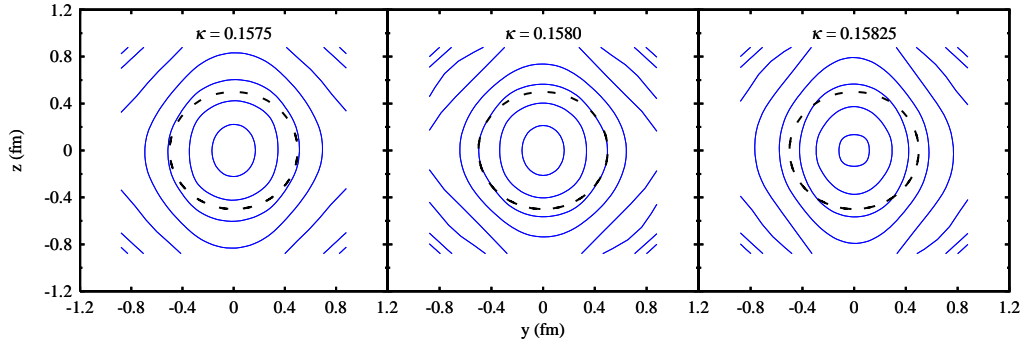


**Figure 3:** Contour plots of the charge distribution of the  $\rho$ -meson projected onto the  $y$ - $z$  plane for all three  $\kappa$  values studied. The dashed circles are to guide the eye.

## 5. Pion and $\rho$ -meson form factors

Form factors can be accurately extracted using four-point functions by taking the Fourier transform of  $G_h^{j\sigma}(\vec{x}, t_1, t_2)$  and allowing large time separations between the current insertions,  $t_2 - t_1$ . Therefore the extraction of form factors requires larger temporal extension than the equal time density-density correlators. Methods to suppress excited state contributions are therefore of crucial importance here. Gaussian smearing combined with HYP smearing achieves ground state dominance as early as three time slices. Taking the Fourier transform of the pion four-point correlator we obtain

$$G_\pi^{j_0}(\vec{p}; t_1, t_2) \xrightarrow[t_1 - t_0 \gg 1, t - t_2 \gg 1]{t_2 - t_1 \gg 1} |\langle \chi_{j_0} | \pi(0) \rangle|^2 \frac{|\langle \pi(0) | j_0 | \pi(\vec{p}) \rangle|^2}{8m_\pi^2 E(\vec{p})} e^{-E(\vec{p})(t_2 - t_1)} e^{-m_\pi(t - (t_2 - t_1) - t_0)}$$

$$= |\langle \chi_\gamma | \pi(0) \rangle|^2 \frac{|(E(\vec{p}) + m_\pi) F_\pi(Q^2)|^2}{8m_\pi^2 E(\vec{p})} e^{-E(\vec{p})(t_2-t_1)} e^{-m_\pi(t-(t_2-t_1)-t_0)}, \quad (5.1)$$

where  $F_\pi$  is the pion form factor and  $Q^2$  is the Euclidean momentum transfer squared. The time dependencies and overlaps cancel by dividing with an appropriate combination of two-point functions:

$$R_\gamma^{j^0}(\vec{p}; t_1, t_2) = \frac{\sqrt{4E(\vec{p})m_\pi}}{E(\vec{p}) + m_\pi} \sqrt{\frac{G_\gamma^{j^0}(\vec{p}; t_0, t_1, t_2, t) G_\gamma(\vec{p}, t_1 - t_0)}{G_\gamma(\vec{p}, t_2 - t_0) G_\gamma(\vec{0}, t - (t_2 - t_1) - t_0)}} \quad (5.2)$$

where  $G_\gamma(\vec{p}, t)$  is the pion two-point function at momentum  $\vec{p}$ . We search for a plateau of  $R_\gamma^{j^0}(\vec{p}; t_1, t_2)$  by varying the time difference  $t_2 - t_1$ , as shown in Fig. 4. We perform the calculation for two source - sink separations, namely  $(t - t_0)/a = 14$  and 16 to check that we have ground state dominance. As can be seen, we obtain consistent plateau values for both source - sink separations.

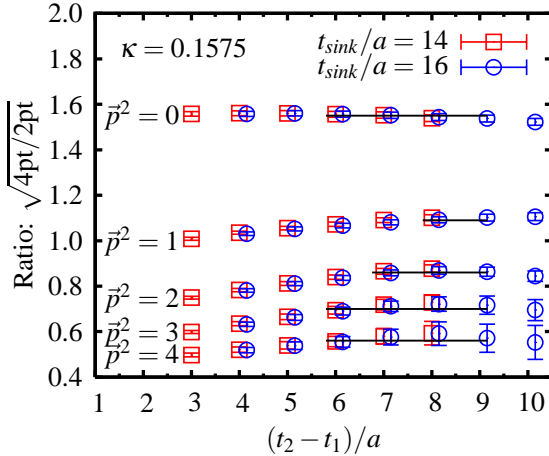


**Figure 4:**  $R_\gamma^{j^0}(\vec{p}; t_1, t_2)$  versus  $(t_2 - t_1)/a$  for  $\kappa = 0.1575$ . The range used for the fit is shown by the length of the lines.

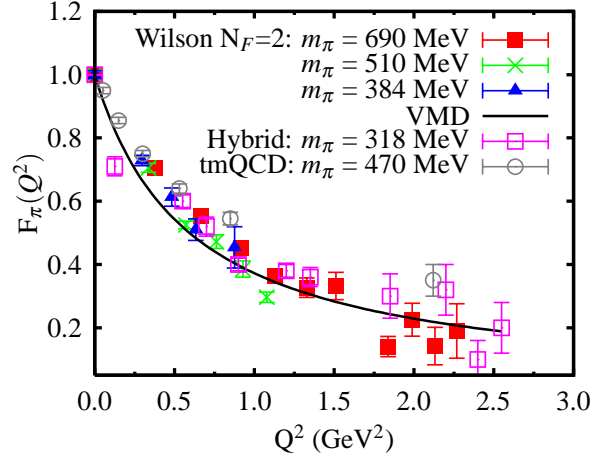


**Figure 5:** The pion form factor for three  $\kappa$ -values. We compare with results using the hybrid approach from [10] and twisted mass results from [6].

In Fig. 5 we show the pion form factor for three  $\kappa$ -values compared with recent results obtained using three-point functions. Results in the hybrid approach, that uses dynamical staggered sea quarks and domain wall valence quarks, are obtained using sequential inversions to compute the three-point function [10]. Results with dynamical twisted mass fermions, on the other hand, use the one-end trick to compute the three-point function [6]. Our results compare very well to those obtained in the latter case, which is closest to our approach. Assuming vector meson dominance and taking  $m_\rho = 0.77$  GeV we obtain the curve shown, for reference, in Fig. 5.

The  $\rho$ -meson has a Coulomb,  $G_C$ , a magnetic,  $G_M$  and a quadrupole,  $G_Q$  form factor. They can be parametrized in terms of  $G_1$ ,  $G_2$  and  $G_3$  as

$$G_Q = G_1 - G_2 + \left(1 + \frac{Q^2}{4M^2}\right) G_3, \quad G_M = G_2, \quad G_C = G_1 + \frac{2}{3} \frac{Q^2}{4M^2} G_Q$$

One can find combinations between initial and final  $\rho$  polarizations and insertion directions ( $\sigma$ ) that isolate individual form factors and for which decay to a pion is forbidden. Here we shall

demonstrate the method by showing preliminary results for  $G_1$ . As for the case of the pion form factor,  $G_1$ , can be extracted using only  $j_0$ :

$$G_{\gamma}^{j_0}(\vec{p}_\perp; t_1, t_2) = \frac{\lambda^2(\vec{0})}{8M^2 E(p_\perp)} (E(p_\perp) + M)^2 G_1^2(Q^2) e^{-M(t-(t_2-t_1)-t_0)} e^{-E(p_\perp)(t_2-t_1)} \quad (5.3)$$

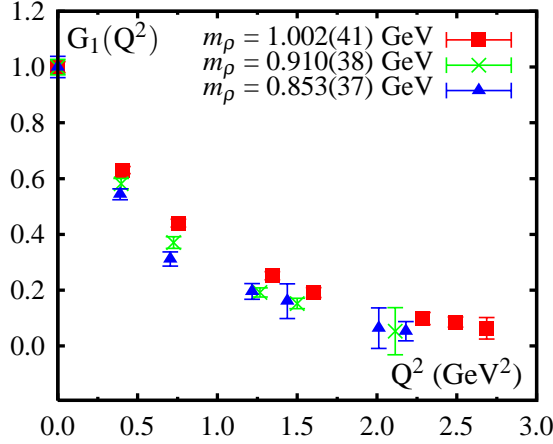


**Figure 6:**  $G_1$  as a function of the momentum transfer  $Q^2$  for three  $\kappa$  values.

where  $\langle \Omega | \chi_{\gamma_k} | \rho(\vec{p}, s) \rangle = \lambda(\vec{p}) \epsilon_k(\vec{p}, s)$ ,  $\sum_s \epsilon_k(\vec{p}, s) \epsilon_{k'}^*(\vec{p}, s) = g_{kk'} - \frac{p_k p_{k'}}{M^2}$  and  $\vec{p}_\perp$  is a momentum perpendicular to the  $k$  direction. As in the case of the pion form factor, we construct an appropriate ratio and search for a plateau in  $t_2 - t_1$ . Results for  $G_1$  are shown in Fig. 6. They carry small statistical errors demonstrating the applicability of the method for the extraction of the  $\rho$ -meson form factors. An analysis to extract all three form factors and subsequently derive physical quantities is in progress.

## 6. Conclusions

We have shown that the one-end trick can be applied to evaluate accurately four-point functions. Using this approach, the density-density correlators are computed to sufficient accuracy to show that the  $\rho$ -meson is deformed. We also obtain accurate results for the pion form factor that compare favorably to the accuracy obtained using the one-end trick to compute the three-point function. The advantage of using four-point functions is that only one set of inversions is needed for all momentum transfers, unlike in the case of three-point functions where one needs new inversions for each value of the momentum transfer. Preliminary results on the  $\rho$ -meson form factor,  $G_1$ , carry small statistical errors demonstrating the applicability of the method also in the calculation of the form factors of the  $\rho$ -meson.

## References

- [1] C. Alexandrou, Ph. de Forcrand and A. Tsapalis, *Phys. Rev. D* **66** (2002) 094503.
- [2] C. Michael and J. Peisa, *Phys. Rev. D* **58** (1998) 034506.
- [3] C. Alexandrou, P. Dimopoulos, G. Koutsou and H. Neff, *PoS (LAT2005)* 030.
- [4] C. Alexandrou, G. Koutsou and H. Neff, *PoS (LAT2006)* 113.
- [5] C. McNeile and C. Michael, *Phys. Rev. D* **73** (2006) 074506.
- [6] S. Simula *et al.*, *PoS (LAT2007)* 374.
- [7] J. Foley *et al.*, *Comput. Phys. Commun.* **172** (2005) 145.
- [8] B. Orth, T. Lippert and K. Schilling, *Phys. Rev. D* **72** (2005) 014503.
- [9] C. Urbach, K. Jansen, A. Shindler and U. Wenger, *Comput. Phys. Commun.* **174** (2006) 87.
- [10] F. Bonnet *et al.*, *Phys. Rev. D* **72** (2005) 054506.